Formation and control of electron molecules in artificial atoms: Impurity and magnetic-field effects

Constantine Yannouleas and Uzi Landman

School of Physics, Georgia Institute of Technology, Atlanta, Georgia 30332-0430
(Received 2 November 1999; revised manuscript received 3 March 2000)

Interelectron interactions and correlations in quantum dots can lead to spontaneous symmetry breaking of the self-consistent mean field, resulting in the formation of Wigner molecules. With the use of spin-and-space unrestricted Hartree-Fock (sS-UHF) calculations, such symmetry breaking is discussed for field-free conditions, as well as under the influence of an external magnetic field. Using as paradigms impurity-doped (as well as the limiting case of clean) two-electron quantum dots (which are analogs to heliumlike atoms), it is shown that the interplay between the interelectron repulsion and the electronic zero-point kinetic energy leads, for a broad range of impurity parameters, to the formation of a singlet ground-state electron molecule, reminiscent of the molecular picture of doubly excited helium. A comparative analysis of the conditional probability distributions for the sS-UHF and exact solutions for the ground state of two interacting electrons in a clean parabolic quantum dot reveals that both of them describe the formation of an electron molecule with similar characteristics. The self-consistent field associated with the triplet excited state of the two-electron quantum dot (clean as well as impurity doped) exhibits a symmetry breaking of Jahn-Teller type, similar to that underlying formation of nonspherical open-shell nuclei and metal clusters. Furthermore, impurity and/or magnetic-field effects can be used to achieve controlled manipulation of the formation and pinning of the discrete orientations of the Wigner molecules. Impurity effects are futher illustrated for the case of a quantum dot with more than two electrons.

I. INTRODUCTION

Two-dimensional (2D) quantum dots (QD's), created at semiconductor interfaces with refined control of their size, shape, and number of electrons, are often referred[1–3] to as ''artificial atoms.'' This analogy suggests that the physics of electrons in such manmade nanostructures is closely related to that underlying the traditional description[4] of natural atoms (pertaining particularly to electronic shells and the Aufbau principle), where the electrons are taken[5] to be moving in a spherically averaged effective central mean field (CMF). However, using as paradigms impurity-doped (as well as the limiting case of clean) two-electron QD ($2e$ QD) analogs to He-like atoms, we show that the interplay between the interelectron repulsion (Q) and the electronic zero-point kinetic energy (K) may lead, for a broad range of impurity parameters, to spontaneous symmetry breaking (SB) of the self-consistent mean field, resulting, at zero magnetic field ($B = 0$), in the formation of a singlet ground-state electron molecule. Such SB is beyond the CMF picture and, while negligible in the ground state of the He atom (whose study was central to the development of the quantum theory of matter due to the failure of the Bohr-type models[6]), it is similar in nature to the SB found[6] in the 1970s in doubly excited He, where the formation of an e-He^{2+}-e ''triatomic'' molecule was invoked. Furthermore, we show that symmetry breaking at $B = 0$ of the self-consistent field associated with the triplet excited state of the $2e$ QD originates from a Jahn-Teller distortion of the CMF, similar to that underlying formation of nonspherical open-shell nuclei[7,8] and metal clusters.[9,10]

Along with a unification of concepts pertaining to spontaneous SB in a variety of finite fermionic systems (from nuclei, metal clusters, and natural atoms, to 2D QD's), we demonstrate the ability to control the orientation and to manipulate (i.e., to enhance, but also to counteract and even to void) the formation of the electron molecules in $2e$ QD's via impurity and/or magnetic-field effects. The ability to control the orientation of the electron molecule may in principle open new possibilities for designing ''on-off'' (i.e., switching between two discrete states) devices, which eventually may be employed in applications of QD's as nanoscale logic gates[11] (the effect of impurities on the structure of multielectron molecules in QD's with more than two electrons is further illustrated in Appendix A).

That electrons in extended media may undergo crystallization at low densities, when Q dominates over K, was predicted[12] by Wigner in 1934. Such Wigner crystallization in clean QD's results in the formation of electron molecules[13–16] [also referred to as Wigner molecules (WM's)], which are associated with spontaneous SB, where the symmetry of the ground state, calculated at the mean-field (self-consistent-potential) level, is found to be lower than that of the exact Hamiltonian describing the system.[17–19] In clean QD's, formation[20] of WM's is controlled[16,21] by the parameter $R_W = Q/K$. For a parabolic confinement (with frequency ω_0) at $B = 0$, it is customary to take $Q = e^2/\kappa l_0$ and $K \equiv \hbar \omega_0$, where κ is the dielectric constant, and $l_0 = (\hbar/m^* \omega_0)^{1/2}$ is the spatial extent of the lowest state's wave function of an electron with an effective mass m^*; WM's occur[16] for $R_W > 1$, corresponding to much higher electron densities[15,16] than those predicted for WC in an infinite 2D medium.[22]

The many-body Hamiltonian for a QD with N_e electrons can be expressed as a sum of a single-particle part and the

two-particle interelectron Coulomb repulsion:

$$\mathcal{H} = \sum_{i=1}^{N_e} H(i) + \sum_{i=1}^{N_e} \sum_{j>i}^{N_e} \frac{e^2}{\kappa r_{ij}}. \tag{1}$$

The contributions to the single-particle part are written as

$$H(i) = H_0(i) + H_B(i) + V_I(i), \tag{2}$$

and they contain a term describing the motion of an electron in a 2D parabolic confinement, i.e., $H_0(i) = \mathbf{p}_i^2/2m^* + m^*\omega_0^2(x_i^2 + y_i^2)/2$, where ω_0 is the frequency of the 2D isotropic harmonic confining potential. Magnetic-field effects are included in $H_B(i) = [(\mathbf{p}_i - e\mathbf{A}_i/c)^2 - \mathbf{p}_i^2]/2m^* + g^*\mu_B\mathbf{B}\cdot\mathbf{S}_i/\hbar$, where the vector potential, $\mathbf{A}_i = B(-y_i/2, x_i/2, 0)$ is taken in the symmetric gauge, and the last term is the Zeeman interaction with an effective factor g^*, $\mathbf{S}_i$ is the electron spin, and μ_B the Bohr magneton. To include the effect of (Coulombic) impurities, we added to $H(i)$ the term $V_I(i) = (e/\kappa)\Sigma_l\mathcal{Q}_l/|\mathbf{r}_i - \mathcal{R}_l|$ ($i = 1, \dots, N_e$), where $\mathcal{Q}_l$ is the charge of the lth impurity located at $\mathcal{R}_l = (x_l, y_l, d_l)$; such impurities, which in general may be situated out of the 2D plane of the QD (that is $d_l \neq 0$), may correspond to implanted atoms (donors or acceptors) or represent a fabricated, controllable voltage gate.

A clean QD (that is with $\mathcal{Q}_l = 0$ in the above Hamiltonian) may be regarded as a realization of the Thomson atom, as are jellium models of metal clusters,[10] where the positive charge is uniformly distributed; in the $2e$ Thomson QD (TQD), the confinement to the 2D plane is modeled by a parabolic potential. On the other hand, a QD analog of the Rutherford model of the atom (RQD), where the positive charges are grouped in a single nucleus, can be achieved through the introduction of a central attractive impurity (in addition to the harmonic confinement).

The presence of many free parameters in Eqs. (1) and (2) results in a plethora of possible case studies generated by varying the material-dependent parameters (κ and m^*), the harmonic confinement ω_0 and the magnetic field B, as well as the number of impurities l, their charges $\mathcal{Q}_l$, and positions $\mathcal{R}_l$. In this paper, we have chosen to discuss the following three representative classes of cases at a specific value of $R_W = 2.39$, which is sufficiently high so that the electrons form[16] a WM in the case of a clean QD, thus allowing for systematic investigations of the effects of impurities on the formation, orientational pinning, and structural distortions of the electron molecules (for the other parameter values used throughout this paper, see Ref. 23). The three representative classes, which we discuss, are (i) a $2e$ TQD at $B = 0$ in the presence of two off-centered impurities situated on both sides of the dot (Sec. II); (ii) a $2e$ RQD (with a single attractive central impurity) in the presence of an applied magnetic field (for both the cases of a weak and a strong field, Sec. III); and (iii) a QD with eight electrons at $B = 0$ and a single impurity with varying strength, polarity, and location (Appendix A).

For the case of a clean $2e$ QD, with the Hamiltonian given by Eqs. (1) and (2) with $N_e = 2$ and $V_I = 0$, the exact solution can be found quite easily,[24–28] owing to the separability of the Schrödinger equation in the center-of-mass and relative coordinates; in the presence of impurities, separabil-

ity is lost, and finding an exact solution[29] becomes significantly more complicated (even for two electrons in the presence of a central impurity). Therefore, and also in order to expound the physical principles underlying spontaneous symmetry breaking in QD's, we will mostly use in the following (Secs. II and III and Appendix A) the self-consistent spin-and-space unrestricted Hartree-Fock (sS-UHF) method[30] which, unlike the restricted HF (RHF) method,[31,32] allows for the formation of broken-symmetry states (of lower energy than those obtained via the RHF method). This sS-UHF method, which we introduced for studies of QD's in Ref. 16, employs N_e (where N_e is the number of electrons) orbital-dependent, effective (mean-field) potentials, and it differs from the usual[33] RHF method in two ways: (i) it relaxes the double-occupancy requirement, namely, it employs different spatial orbitals for the two different (i.e., the up and down) spin directions [thus the designation "spin (s) unresricted"]; and (ii) it relaxes the requirement that the electron orbitals be constrained by the symmetry of the external confining field [thus the designation "space (S) unrestricted"].

Subsequent to our discussion of symmetry breaking and formation of electron molecules in the framework of the sS-UHF method, we elaborate in Sec. IV on the connection between the symmetry-broken sS-UHF solution and the exact one in the case of a clean $2e$ QD with $B = 0$. In particular, analysis of the exact solution using the conditional-probability-distribution technique[34] reveals the formation of an electron molecule, in agreement with the sS-UHF result.

II. THOMSON QUANTUM DOT WITH OUTSIDE IMPURITIES

To introduce some of the principal physical and methodological issues pertaining to symmetry breaking and formation of Wigner molecules in finite fermion systems, we first discuss the $2e$ TQD at $B = 0$ [we remind the reader that a sufficiently high value of $R_W(=2.39)$ was chosen, such that the QD is in the regime where the two electrons form a WM; for the other parameters used throughout this paper, see Ref. 23]. The single-particle wave functions (modulus square) and total electron densities displayed in Fig.1 are taken from calculations for the $2e$ TQD in the presence of two attractive impurities ($\mathcal{Q}_1 = \mathcal{Q}_2 = -1e$, represented in the figure by filled dots on the two sides of the QD) located symmetrically about the center of the QD at $(x, y, z) = (\pm 60, 0, 10)$ nm, with the strength and location of the impurities purposefully chosen such that they will not affect the nature of the electronic ground states (for the same QD but without the impurities), except for orientational pinning in the case of symmetry-broken states (see below).

First constraining the solution to maintain the symmetry of the Hamiltonian, in conjunction with double occupancy of the HF orbitals by electrons of opposite spins [that is through the use of the RHF method with input trial electron densities satisfying the symmetry of the external potentials[31]], the resulting symmetry-adapted (SA) self-consistent singlet ($\mathcal{S}$) orbitals and corresponding total-density distributions exhibit, as expected, an almost circular symmetry with minimal elliptical distortions (due to the impurities) [see Fig. 1(a)];
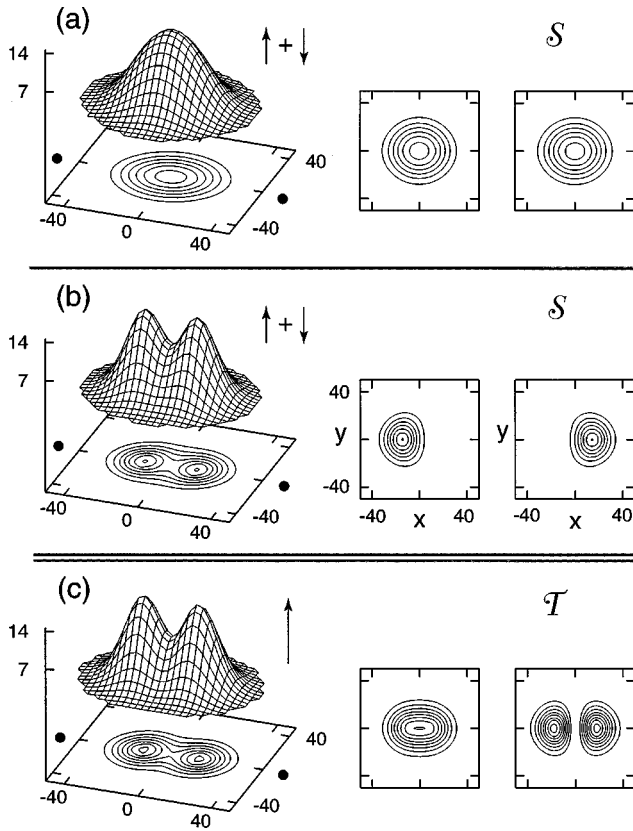
FIG. 1. Total electron densities (left frame in each panel) and contours of modulus square of the individual orbitals (right frames) for the clean (Thomson) $2e$ TQD at $B=0$, in the presence of two attractive ($Q_1 = Q_2 = -1e$) impurities whose projected positions on the QD plane (xy) are denoted by filled circles. (a) The symmetry-adapted (RHF) singlet (S). The energy of the SA singlet is *higher* by 1.34 meV than that of the corresponding triplet, manifesting a shortcoming of the RHF method. (b) The sS-UHF Wigner-molecule singlet, orientationally pinned along the interimpurity axis and exhibiting localized orbitals, one to the left and the other to the right of the QD middle; note the lack of reflection symmetry of the individual orbitals about the mirror (yz) plane normal to the interimpurity axis and passing through the QD's center. When the WM singlet is rotated by $\pi/2$, the energy of the system rises by 0.58 meV. (c) The triplet (T) state with an elliptically deformed s-like orbital and a p_x-like orbital, orientationally pinned by the impurities. The energy of the symmetry-broken singlet in (b) is *lower* by 0.28 meV than that of the triplet in (c), compared to 0.43 meV for the TQD without pinning impurities. Distances are in nm and the electron densities in 10^{-4} nm^{-2}. The parameters characterizing the QD shown here are those given in Ref. 23.

without the impurities, the SA singlet is perfectly circularly symmetric.

However, increasing the variational freedom through removal of the spatial symmetry and double-occupancy constraints via the use of the sS-UHF method results in a symmetry-broken singlet ground state of lower energy, that is, to the formation of a WM characterized by localized orbitals with the "bond length" (distance between the maxima in the total electronic distribution) equal to 29 nm [see Fig. 1(b)]; the energy of this state is lower by 1.62 meV than that of the SA solution [Fig. 1(a)]. This lowering of the ground-state energy reflects a gain in the correlation energy (for the definition of correlation energy, see Sec. IV below). Note

that the $2e$ WM is orientationally pinned along the interimpurity axis. Similar formation of a WM also occurs for a $2e$ TQD without the pinning impurities (with an energy gain of 1.32 meV compared to the corresponding SA solution). However, in the absence of pinning, the formation of the WM is accompanied by orientational degeneracy[35] (that is there is an infinite manifold of rotationally degenerate sS-UHF ground states).

The formation of a fermionic molecule, associated with electron localization, in the ground state of a QD under magnetic-field-free conditions does not have an analog within the framework of the traditional models of atomic structure.[4] However, the physics underlying this phenomenon, which is a manifestation of SB resulting from strong electronic correlations (also see Sec. IV below), closely resembles that found in doubly excited two-electron atoms. Indeed, spectroscopical studies on doubly excited helium atoms revealed rovibrational bands which were interpreted, borrowing from models developed in the context of nuclear and molecular physics, by invoking the formation of a "triatomic" molecule comprised of the two localized electrons and the He^{2+} nucleus (α particle), with the collinear configuration being of particular significance.[6]

The first electronically excited state of the $2e$ TQD is the triplet T state (with the spins of the two electrons parallel to each other), whose total electron density distribution [Fig. 1(c), left] resembles that of the ground-state singlet [Fig. 1(b), left]. However, the individual electronic wave functions in the T state differ in character from those of the S state [compare right panels in Figs. 1(c) and 1(b)], with the lower-energy one being s like (but elliptically distorted), and the other being a p-like orbital oriented by the impurities along the x axis. Note that the T state has the symmetry of the Hamiltonian, including the two pinning impurities (that is, here the sS-UHF solution coincides with the symmetry-adapted one). The same orbital characters are also obtained in the absence of pinning impurities, but without a preferred orientation. In this case, however, the character of the T state is a result of spontaneous SB, with an energy gain of 0.09 meV compared to the corresponding SA (circular) solution. Underlying the type of spontaneous SB in the (open-shell) T state of the $2e$ TQD is the Jahn-Teller (JT) effect,[36] where a lowering of the total energy is achieved via mixing of the twofold degenerate $m = +1$ (p_+) and $m = -1(p_-)$ angular momentum states, concomitant with a deformation of the self-consistent potential away from circular symmetry.[37] To distinguish such electron molecules from the WM discussed above for the closed-shell singlet state (whose formation is driven by the dominance of the electron-electron repulsion), we refer to them as JT electron molecules (JTEM's). Such spontaneous SB via JT distortions is familiar from studies of the rotational spectra of open-shell nuclei[7,8] and from investigations of shape deformations of open-shell metal clusters.[9,10]

Similar calculations for the $2e$ TQD, but with repulsive pinning impurities (that is $Q_1 = Q_2 = +1e$) yield, for the singlet ground state, qualitatively similar results (with different values for the energies), but with the important distinction that now the pinned orientation of the WM is rotated by $\pi/2$ compared to the $Q_1 = Q_2 = -1e$ case (i.e., the "intramolecular" axis of the WM is oriented normal to the interimpurity

axis). Consequently, through a variation of the sign (polarity) of the impurity gate voltages, one may ''flip'' the orientation of the WM, and with it the direction of the polarization of the electronic charge distribution in the QD. In this way, the formation of WM's in QD's, and the ability to control their discrete orientations via pinning voltage gates, may serve as a method for the creation of on-off information storage cells and nanoscale logic gates.[11]

III. RUTHERFORD QUANTUM DOT

Next we examine the properties of a $2e$ Rutherford QD (RQD), that is, a $2e$ QD with a central attractive impurity. The sS-UHF singlet and triplet electronic orbitals corresponding to a $2e$ RQD for $B=0$ with a single impurity ($\mathcal{Q} = -2e$) located at $(0,0,10)$ nm are shown in Figs. 2(b) and 2(c) respectively. They exhibit WM symmetry breaking and JT-distortion features similar to those found for the $2e$ TQD [compare Figs. 1(b) and 1(c)], but with a reduced WM bond length and a more compact triplet. The ''strength'' of the SB depends, of course, on the impurity charge $\mathcal{Q}$ and/or its distance d from the QD plane. For example, for $\mathcal{Q}=-1e$ and $d=0$ (and for an arbitary position of the impurity inside the QD), no symmetry breaking was found by us due to the strong trapping by the impurity of the two electrons which occupy circularly symmetric orbitals, resembling the behavior of the ground state of the natural He atom.[38] We also remark that for the case described in Figs. 2(b) and 2(c) both electrons are slightly trapped by the impurity potential for the $\mathcal{S}$ state, while for the $\mathcal{T}$ state the s-like electron is strongly trapped and the p-like electron occupies a much less bound orbital. Note that here, as with the case of a clean QD, the singlet WM and the JT-distorted triplet are free to rotate in the plane of the QD, since there are no off-centered pinning impurities.

The large physical size of QD's makes them ideally suited for investigations of magnetic-field effects and controlled manipulations. To illustrate such effects, in Fig. 2(a) we display the magnetic-field-induced variation of the total energies of the $\mathcal{S}$ and $\mathcal{T}$ states in the $2e$ RQD (qualitatively similar behavior is found also for the $2e$ TQD). As seen, the energy of the singlet state increases and that of the triplet state decreases with increasing B; for fields $B<B_1$ (0.2 T), the variation of the energy of the $\mathcal{T}$ (the slope of the curve) is smaller than that for $B>B_1$ [see the inset in Fig. 2(a)]. Furthermore, at a critical value $B_c=2.8$ T [marked by a down arrow in Fig. 2(a)], the energies of the two states cross, and from then on the triplet lies below the singlet. For the singlet, the broken-symmetry WM state [Fig. 2(b)] is maintained under the influence of the applied magnetic field in the range considered in Fig. 2(a), with the increase in the magnetic-field strength leading to further shrinkage of the bond length of the WM accompanied by an overall increase of the energy of the $\mathcal{S}$ state[39] [see Fig. 2(a)].

The influence of the magnetic field on the triplet state is more subtle. As aforementioned, at $B=0$ the symmetry of the $\mathcal{T}$ state is broken by the JT effect, involving a mixing of the $m=\pm 1$ degenerate angular momentum orbitals (see Ref. 37). On the other hand, the magnetic field lifts the degeneracy of these p_+ and p_- states (without mixing them), and this effect competes with the JT distortion. For small enough
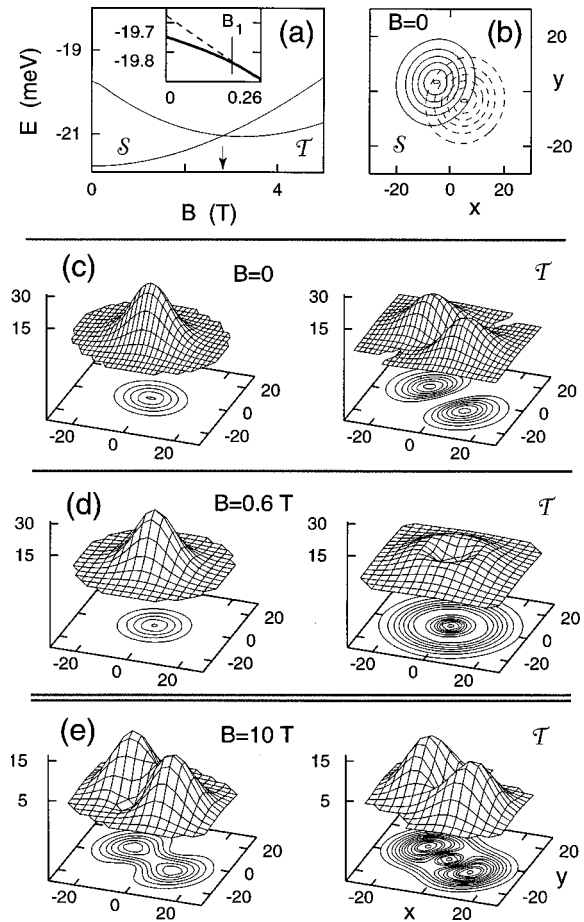

FIG. 2. (a)–(d) Energetics and individual orbitals (modulus square) from sS-UHF calculations for the $2e$ (Rutherford) RQD, with a central impurity $\mathcal{Q}=-2e$ at $(0,0,10)$ nm. Energies (in meV) of the $\mathcal{S}$ and $\mathcal{T}$ states vs B (in T), crossing at $B_c=2.8$ T (marked by an arrow), are shown in (a). An expanded view of the energy of the $\mathcal{T}$ state for small fields, exhibiting a transition from the spontaneous JT regime to a circular symmetric state at $B>B_1(B_1=0.2$ T), is shown in the inset; also included is the energy of the SA solution (dashed curve). At $B=0$, contours of the orbitals of the two electrons for the WM singlet are shown (superimposed on each other) in (b), with one of the orbitals depicted by a solid line and the other by a dashed line. The orbitals for the spontaneously JT-distorted triplet at $B=0$ are shown in the two panels of (c). For the singlet, the energy gain due to SB (that is lowering of the total energy with respect to the symmetry-adapted RHF state) is 0.39 meV and the energy gain due to the JT distortion of the triplet is 0.07 meV; the energy difference between the $\mathcal{T}$ and $\mathcal{S}$ states is 2.01 meV. The transition to a circular symmetric triplet is illustrated for $B=0.6$ T in (d). (e) Individual orbitals for the symmetry-broken ground-state triplet of the clean (Thomson) $2e$ TQD at $B=10$ T. Under the same conditions, the ground state triplet in the $2e$ RQD remains circularly symmetric. Distances in nm and orbital densities in 10^{-4} nm^{-2}. Note the different length scales of the (x,y) axes in (b)–(e) compared to those in Fig. 1. The parameters characterizing the QD's shown here are those given in Ref. 23.

fields [$B<B_1$; see the inset in Fig. 2(a)] the JT effect prevails, and thus the orbitals and electron densities remain similar to those shown in Fig. 2(c), and they maintain an orientational degeneracy in the plane. At stronger fields ($B>B_1$), the lifting of the energetic degeneracy of the p_+ and p_- states overcomes the JT effect, and the second electron

populates the lower of these two orbitals. As a result, circular symmetry is recovered, as illustrated in Fig. 2(d).

The overall decrease with B of the energy of the $\mathcal{T}$ state relative to the $\mathcal{S}$ state is due to enhanced stabilization by the (parallel-spin) exchange energy in the former, reduced Coulomb repulsion between the electrons occupying s- and p-like orbitals, and a quenching of the kinetic energy of the p-like orbital by the magnetic field.[39] This effect increases with B, and at $B \geq B_c$ the $\mathcal{T}$ state becomes the ground state [see Fig. 2(a)]. Note that this transition is driven primarily by the interelectron repulsion, and not by the interaction of the electrons' moments with the magnetic field (see Ref. 2, and references therein); for our system, the Zeeman splitting energy is 0.026 meV/T. At even larger fields, the Coulomb repulsion between the electrons increases (due to the shrinking of the orbitals), resulting in an ascending trend of the energy of the $\mathcal{T}$ state, which remains, however, lower than the singlet state. A similar scenario is found also for the TQD (without pinning impurities).

In light of previous findings[13,14] pertaining to the formation of fully spin-polarized symmetry-broken states in clean QD's (TQD's) at high magnetic fields, it is pertinent to inquire whether the circular symmetry found for the $\mathcal{T}$ state of the $2e$ RQD for $B_1 < B < 5$ T will also be broken at higher fields. For the clean $2e$ TQD, we verified that indeed an orientationally degenerate electron molecule [with the molecular orbitals of the electrons distributed about the two molecular centers; see Fig. 2(e)] formed at sufficiently high B (e.g., $B = 10$ T). Such an electron molecule is akin[40] to the JTEM discussed above in the context of triplet state for $B = 0$. Interestingly, such a reemergence of a JTEM structure does not occur at these conditions for the $2e$ RQD studied here, due to the enhanced gap between the p_+ orbital and the strongly trapped s orbital. This provides an additional venue for impurity-assisted manipulation and design of the electronic properties of QD's.

IV. CONNECTION TO THE EXACT SOLUTION

As mentioned earlier, for $R_W > 1$, the sS-UHF approach applied to QD's yields *approximate* ground-state solutions which violate the symmetries of the original many-body Hamiltonian, e.g., the spontaneous breaking of rotational symmetry discussed in Secs. II and III for a circularly symmetric clean QD (i.e., a TQD) or one with a central impurity (i.e., a RQD). At a first glance, this situation may appear puzzling, but it is not unique in the context of many-body theory of finite fermionic systems. Indeed, a similar situation was encountered in nuclear physics in the 1950s, when it was discovered that open-shell nuclei carried permanent quadrupole moments and that many of them exhibited well-developed rotational spectra (i.e., they behaved like rigid rotors). The explanation for these experimental findings was formulated in the framework of breaking of the rotational symmetry associated with nuclear deformations of the Jahn-Teller type, and it led to several celebrated models and semiempirical methods, i.e., the particle-plus-rotor model of Bohr and Mottelson,[41] the modified-anisotropic-oscillator model of Nilsson,[42] and the Strutinsky shell-correction method.[43] In the language used by us here, this means that at the microscopic level the breaking of the rotational symmetry had to

be accounted[44] for via space (S)-UHF methods (that is, allowing the spatial-orbital solutions of the Hartree-Fock equations to assume symmetries lower than those of the underlying many-body Hamiltonian).

Starting with Peierls and Yoccoz[45] (see also Peierls and Thouless[46]), numerous theoretical investigationss addressed the connection of the broken-symmetry HF solution to the exact solution, and led to the theory of *restoration-of-symmetry* via projection techniques.[47] The central physical ingredient of the projection technique rests with the observation that a HF solution which breaks rotational symmetry is not unique, but belongs to an infinitely degenerate manifold of states with different spatial orientation. A proper linear combination of the HF determinants in such a manifold yields multideterminental states with good *total* angular momenta that are a better approximation to the exact solution. For a comprehensive review on restoration of symmetry in the context of nuclear many-body theory, we refer the reader to the book by Ring and Schuck mentioned in Ref. 35 (see also Ref. 48, where the principles of restoration of rotational symmetry are discussed in the two-dimensional case).

The restoration of symmetry via projection techniques in the case of sS-UHF solutions describing 2D QD's will be presented in a future publication. In this section, we found it more convenient to discuss the connection between the sS-UHF and the exact solutions by taking advantage of the simplicity of solving the exact problem at $B = 0$ for two electrons interacting via the Coulomb force and confined by an external parabolic confinement without impurities (a clean QD). Indeed, it is well known that, in this case, the exact Schrödinger equation for two interacting electrons is separable in the center-of-mass, $\mathbf{R} = (\mathbf{r}_1 + \mathbf{r}_2)/2$ (with a corresponding mass $\mathcal{M} = 2m^*$), and relative, $\mathbf{r} = \mathbf{r}_1 - \mathbf{r}_2$ (with a corresponding reduced mass $\mu = m^*/2$), coordinates.

To analyze the properties of the exact solutions, two quantities[25,27] have customarily been extracted from the two-body wave function $\Psi(\widetilde{\mathbf{r}}_1, \widetilde{\mathbf{r}}_2)$ [where the tilde denotes both spatial and spin variables, i.e., $\widetilde{\mathbf{r}}_i \equiv (\mathbf{r}_i, s_i)(i = 1, 2)$ (see Appendix B)]: (i) the usual pair-correlation function[49]

$$G(v) = 2\pi \langle \Psi | \delta(\mathbf{r}_1 - \mathbf{r}_2 - \mathbf{v}) | \Psi \rangle; \tag{3}$$

and (ii) the electron density

$$n(v) = \langle \Psi | \sum_{i=1}^{2} \delta(\mathbf{v} - \mathbf{r}_i) | \Psi \rangle. \tag{4}$$

However, for the exact Ψ in the case of a circularly symmetric confinement, both of these quantities also turn out to be circularly symmetric, and thus they do not reveal the full physical picture, the (possible) formation of an electron molecule generated by electron correlations. A more suitable quantity here is the conditional probability distribution (CPD) $\mathcal{P}(\mathbf{v} | \mathbf{r}_2 = \mathbf{v}_0)$ for finding one electron at $\mathbf{v}$ given that the second electron is at $\mathbf{r}_2 = \mathbf{v}_0$. This quantity has been extensively used[34] in the analysis of electron correlations in doubly excited heliumlike atoms, and is defined as

$$\mathcal{P}(\mathbf{v} | \mathbf{r}_2 = \mathbf{v}_0) \equiv \frac{\langle \Psi | \delta(\mathbf{v} - \mathbf{r}_1) \delta(\mathbf{v}_0 - \mathbf{r}_2) | \Psi \rangle}{\langle \Psi | \delta(\mathbf{v}_0 - \mathbf{r}_2) | \Psi \rangle} \tag{5}$$
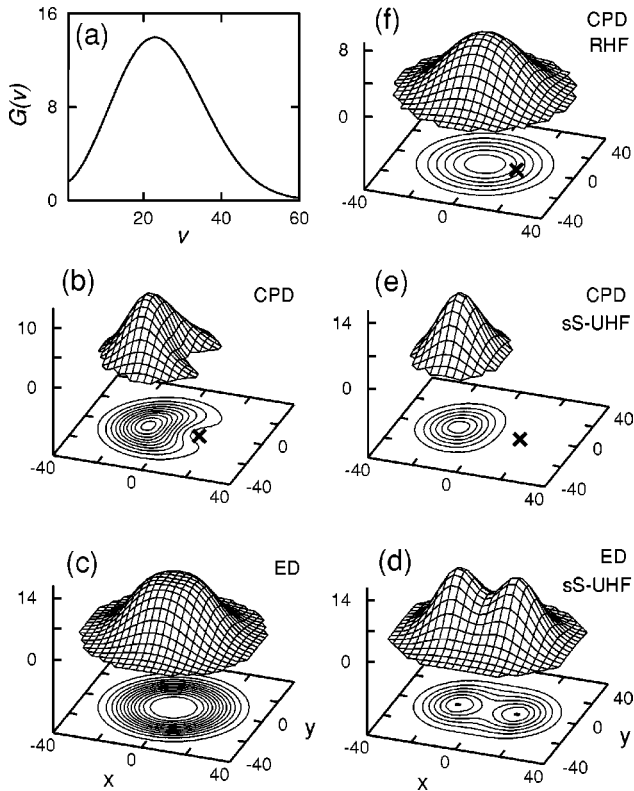
FIG. 3. Ground-state results for a clean $2e$ QD with the parameters given in Ref. 23 and $B=0$; in all cases the ground state is a singlet. (a)–(c) correspond to the exact solution. (a) The pair correlation function $[G(v)$; see Eq. (3)] plotted vs v exhibiting a well-developed depression at $v=0$, with a mean electron-to-electron separation of $2r_0=22.92$ nm. (b) The electron conditional probability distribution [CPD; see Eq. (5)] with $\mathbf{v}_0=(r_0, 0)$ (denoted by a cross), showing formation of a $2e$ electron molecule. (c) The electron density [ED; see Eq. (4)], reflecting the conservation of circular symmetry by the exact two-electron solution. The results displayed in (d) and (e) correspond to calculations using the sS-UHF method. Spontaneous symmetry breaking leading to formation of a $2e$ molecule (with a bond length of $2r_0'=28.16$ nm) is exhibited by the sS-UHF electron density shown in (d). (e) Such an electron molecule is further reflected in the sS-UHF CPD with $\mathbf{v}_0=(r_0',0)$ (denoted by a cross). (f) The CPD with $\mathbf{v}_0=(r_0',0)$ (denoted by a cross) corresponding to the restricted Hartree-Fock (RHF) ground state (i.e., the symmetry-adapted solution) exhibits, as expected, no symmetry-breaking signature. Lengths are in nm, and density functions $[G(v)$, ED's, and CPD's] are in units of 10^{-4} nm^{-2}.

[for details concerning the calculation of the quantities in Eqs. (3)–(5), see Appendix B].

In the left column of Fig. 3, we display the above three quantities for the exact ground state in the case of a parabolic confinement with the same parameters as used throughout this paper (see Ref. 23) and $B=0$. The pair-correlation function in Fig. 3(a) exhibits a well-developed depression at $v=0$, namely, the two electrons on the average keep apart from each other at a distance $2r_0=22.92$ nm. In Fig. 3(b), we plot the CPD with $\mathbf{v}_0=(r_0,0)$ (marked by a cross). It is seen that the maximum probability for finding the second electron occurs at the diametrically opposite point $-\mathbf{v}_0$, in accordance with the picture of an electron molecule presented earlier within the sS-UHF approach. The exact elec-

tron density shown in Fig. 3(c) is circularly symmetric, as expected. Comparing Figs. 3(b) and 3(c), the following interpretation ensues naturally: the CPD in Fig. 3(b) describes the electron molecule in its *intrinsic (body-fixed)* frame of reference, while the electron density in Fig. 3(c) describes the electron molecule in the laboratory frame of reference where rotational and center-of-mass displacements are superimposed upon the intrinsic probability density.

Figure 3(d) displays the electron density for the corresponding sS-UHF ground state. As discussed earlier, the sS-UHF electron density breaks the rotational symmetry, and clearly exhibits the morphology of an electron molecule, unlike the exact one in Fig. 3(c). It is apparent that the sS-UHF electron density corresponds to that in the intrinsic frame of the electron molecule. Restoration of the symmetry via projection techniques will bring the sS-UHF electron density closer to that of the exact solution. As aforementioned, this interpretation is familiar in the context of nuclear calculations, and it is further supported by the CPD calculated with the sS-UHF ground-state [i.e., by using Ψ^{UHF} in Eq. (5), instead of the exact many-body Ψ; see Appendix B], and displayed in Fig. 3(e). Although naturally not identical, the two CPD's (i.e., the exact and the UHF) are of similar nature, and both illustrate graphically the correlation effect associated with electron localization and formation of an electron molecule. We further illustrate this point by contrasting the exact and sS-UHF CPD's with the CPD of the symmetry-adapted RHF ground state, shown in Fig. 3(f). In this latter case, $\Psi^{\mathrm{RHF}}=\psi^{\mathrm{RHF}}(\mathbf{r}_1)\,\psi^{\mathrm{RHF}}(\mathbf{r}_2)\chi(s_1,s_2;S=0)$, with $\psi^{\mathrm{RHF}}(\mathbf{v})$ being the $1s$ orbital of the RHF approximation; as a result, the probability of finding one electron at $\mathbf{v}$ is independent of the position of the second electron, and it is centered about the origin where it achieves its maximum value, as expected from an independent-particle description, i.e.,

$$\mathcal{P}^{\mathrm{RHF}}(\mathbf{v}|\mathbf{r}_2=\mathbf{v}_0)=|\psi^{\mathrm{RHF}}(\mathbf{v})|^2. \qquad (6)$$

Finally it is of interest to examine the energetic aspects of the symmetry breaking. Indeed the energy of the ground-state is $E_{\mathrm{gs}}^{\mathrm{RHF}}=22.77$ meV for the RHF solution, $E_{\mathrm{gs}}^{\mathrm{UHF}}=21.45$ meV for the sS-UHF and $E_{\mathrm{gs}}^{\mathrm{ex}}=19.80$ meV for the exact one. Since the correlation energy is the difference between the RHF solution and the exact energies,[50] one finds $\varepsilon_{\mathrm{gs}}^{\mathrm{corr}}=E_{\mathrm{gs}}^{\mathrm{RHF}}-E_{\mathrm{gs}}^{\mathrm{ex}}=2.97$ meV. Thus the symmetry breaking associated with the sS-UHF solution is able to capture $(E_{\mathrm{gs}}^{\mathrm{RHF}}-E_{\mathrm{gs}}^{\mathrm{UHF}})/\varepsilon_{\mathrm{gs}}^{\mathrm{corr}}=44\%$ of the correlation energy; the remaining amount can be captured through improvements via projection techniques.[51]

V. SUMMARY

The dominance of interelectron interactions and correlations in quantum dots (often referred to as ''artificial atoms'') results in a spontaneous symmetry breaking of the self-consistent mean field, beyond the central-field picture on which the modern understanding of atomic structure has been founded. Indeed, as shown in this paper through spin-and-space unrestricted Hartree-Fock[16,30] many-body calculations, for the singlet ground state of a $2e$ QD, such symmetry breaking and the resulting formation of Wigner molecules do occur for a wide range of system parameters (with or without

impurities) even in the most elementary case of two-electron QD's. Additionally, in the case of fully polarized dots (e.g., the triplet state of a $2e$ QD), the sS-UHF calculations show that similar electron molecules form due to symmetry breaking associated with Jahn-Teller-type distortions.

In spite of the simplicity of the Hamiltonian, correlations in two-electron QD's underlie a remarkably rich and complex physical behavior. As a result, $2e$ QD's can serve as paradigms for a unification of concepts pertaining to spontaneous SB in various finite-fermion aggregates, including nuclei, excited atoms, and clusters.

Furthermore, impurity and/or magnetic-field effects allow for controlled manipulation of the formation and pinning of the discrete orientations of the electron molecules in $2e$ QD's. Such an ability may be employed in future applications of QD's as nanoscale logic cells and information storage elements. Impurity effects were also illustrated for the case of a quantum dot with more than two electrons.

Confirmation of the formation in $2e$ QD's of electron molecules associated with symmetry breaking of the self-consistent field (in the context of sS-UHF calculations) was obtained through an analysis of the exact ground state via the conditional-probability-distribution technique.

APPENDIX A: QD'S WITH MORE THAN TWO ELECTRONS

In the main body of this paper we limited ourselves to the case of $2e$ QD's, since focusing on this elementary case allowed us to better elucidate the intricate physical principles involved in the formation and impurity control of electron molecules in QD's, from both the perspective of the sS-UHF treatment and the exact solution. In this appendix, we will present an example of the many different structural possibilities that can arise when impurities are introduced in a QD with a larger number of electrons. In particular, we consider a QD with eight electrons in the presence of a hydrogeniclike ($d=0$) impurity of variable nominal charge $\mathcal{Q}=qe$ placed at the center (and in one case offcenter) of the QD (for the other input parameters, we use same values as used throughout the text; see Ref. 23). Since this appendix does not intend to present an exhaustive study of larger dots, but simply aims at presenting an illustrative example, we will consider only one spin configuration, i.e., the sS-UHF solutions having four spin-up and four spin-down electrons. However, q will be allowed to take both positive (repulsive) and negative (attractive) values.

Figure 4(a) displays the sS-UHF electron density for a repulsive central impurity [located at $(0,0,0)$] with $\mathcal{Q}=+1e$. It is seen that a Wigner molecule consisting of a single ring with eight electrons [denoted as a $(0,8)$ ring] is formed in this case. For a slightly attractive central impurity with $\mathcal{Q}=-0.2e$, however, a structural change takes place: one electron moves to the center of the dot [see Fig. 4(b)]. Notice that this $(1,7)$ structure agrees with the arrangement found in studies of classical point-charges in a purely ($\mathcal{Q}=0$) har-
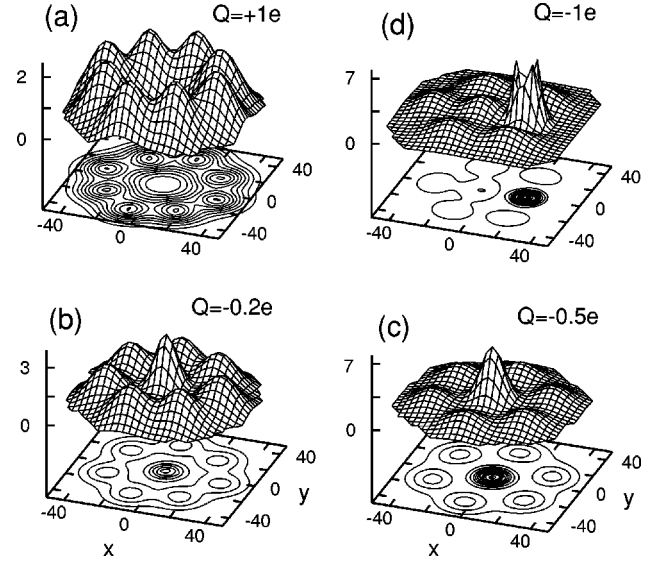

FIG. 4. Electron densities obtained via sS-UHF calculations of a QD containing eight electrons at $B=0$ in the presence of a central [located at $(0,0,0)$ in (a)–(c)] and an off-centerd [located at $(20,0,0)$ nm in (d)] hydrogenic impurity. The parameters characterizing the QD shown here are those given in Ref. 23 and the charge $\mathcal{Q}$ of the impurity is as marked on the figure. All the cases correspond to zero total spin, i.e., $4e$, with spin-up and $4e$ with spin down. For each of the cases, we observe formation of a Wigner molecule, with its structure dependent on the polarity (sign), magnitude, and location of the impuriry. (a) A repulsive central impurity ($\mathcal{Q}=+1e$), resulting in an $8e$ WM with a ring structure and an empty-electron central region, denoted as $(0,8)$. (b) Slightly attractive central impurity ($\mathcal{Q}=-0.2e$) leading to formation of an $(1,7)$ two-ring WM. (c) A stronger attractive central impurity ($\mathcal{Q}=-0.5e$) associated with a $(2,6)$ WM. (d) An off-center attractive impurity ($\mathcal{Q}=-1e$), resulting in a distorted $6e$ WM with two electrons trapped by the impurity. Lengths in nm and electron densities in units of 10^{-3} nm^{-2}.

monic confinement.[20] Increasing the attractive nominal charge to $\mathcal{Q}=-0.5e$ [see Fig. 4(c)] results in a further structural change: the central impurity is now able to trap two electrons, thus leading to a $(2,6)$ arrangement. A further increase of the attractive charge of the impurity to the value $\mathcal{Q}=-1e$ does not produce any qualitative change in the $(2,6)$ arrangement, as long as the impurity remains at the center of the dot. By moving the impurity to an off-center position, however, various structural morphologies can arise, an example of which is presented in Fig. 4(d) for a $\mathcal{Q}=-1e$ impurity located at $(20,0,0)$ nm, forming a highly distorted $(2,6)$ WM (here the first index denotes that two electrons are trapped by the impurity). A further increase in the attractive charge $\mathcal{Q}$ leads to sequential trapping of the remaining six electrons, and to progressive elimination of symmetry breaking, until all eight electrons have been captured by the impurity (also see Sec. III).

APPENDIX B: TWO-ELECTRON WAVE FUNCTIONS AND DEFINITIONS (3)-(5)

1. Exact solution for two electrons

In the case of two interacting electrons confined by a parabolic potential (a clean QD), one can perform a change

of variables to center-of-mass (CM), $\mathbf{R}=(\mathbf{r}_1+\mathbf{r}_2)/2$ and $\mathbf{P}=\mathbf{p}_1+\mathbf{p}_2$, and relative-motion (rm), $\mathbf{r}=\mathbf{r}_1-\mathbf{r}_2$ and $\mathbf{p}=(\mathbf{p}_1-\mathbf{p}_2)/2$, coordinates. Then the two-electron Hamiltonian separates into CM and rm contributions:

$$\mathcal{H}=\mathcal{H}_{\text{CM}}+\mathcal{H}_{\text{rm}}, \tag{B1}$$

with

$$\mathcal{H}_{\text{CM}}=\frac{\mathbf{P}^2}{2\mathcal{M}}+\frac{1}{2}\mathcal{M}\omega_0^2R^2 \tag{B2}$$

and

$$\mathcal{H}_{\text{rm}}=\frac{\mathbf{p}^2}{2\mu}+\frac{1}{2}\mu\omega_0^2r^2+\frac{e^2}{\kappa r}, \tag{B3}$$

where $\mathcal{M}=2m^*, R=|\mathbf{R}|, \mu=m^*/2$, and $r=|\mathbf{r}|$.

The center-of-mass motion associated with the coordinate $\mathbf{R}$ obeys a Schrödinger equation describing the motion of a particle of mass $\mathcal{M}=2m^*$ in a 2D isotropic harmonic potential of frequency ω_0. Here ω_0 is the frequency of the original parabolic confinement, i.e., the interelectron repulsion has no bearing on the center-of-mass motion.

Using dimensionless polar coordinates $U=R/(l_0\sqrt{2})$ and Θ, the center-of-mass wave function can be written as $\Xi(U)e^{iM\Theta}$, with the radial part given by

$$\Xi(U)=C_{NM}U^{|M|}e^{-U^2/2\mathcal{L}_0^2}L_N^{|M|}(U^2/\mathcal{L}_0^2), \tag{B4}$$

where (N,M) are the radial and azimuthal (related to the angular momentum) quantum numbers, respectively, $\mathcal{L}_0=1/2$, the normalization constant $C_{NM}=[2N!4^{|M|+1}/(N+|M|)!]^{1/2}$, and $L_N^{|M|}(x)$ are associated Laguerre polynomials.

Since in the exact problem the Coulomb interaction preserves the rotational symmetry, the radial part of the wave function $\Omega(u)e^{im\theta}/\sqrt{u}$ associated with the relative motion obeys the following one-dimensional Schrödinger equation [in dimensionless polar coordinates $u=r/(l_0\sqrt{2})$ and θ]:

$$\frac{\partial^2\Omega}{\partial u^2}+\left\{\frac{-m^2+1/4}{u^2}-u^2-\frac{R_W\sqrt{2}}{u}+\frac{\varepsilon}{\hbar\omega_0/2}\right\}\Omega=0. \tag{B5}$$

The $1/u$ term results from the interelectron repulsion.

Defining $\widetilde{\mathbf{u}}_i\equiv(\mathbf{u}_i,s_i)$ (where s_i is the spin of the ith electron and $i=1$ and 2), the exact many-body (here two-body) wave function is given by

$$\Psi(\widetilde{\mathbf{u}}_1,\widetilde{\mathbf{u}}_2)=\Phi(\mathbf{u}_1,\mathbf{u}_2)\chi(s_1,s_2)$$

$$=\frac{1}{2\pi}\frac{\Omega(u)}{\sqrt{u}}e^{im\theta}\Xi(U)e^{iM\Theta}\chi(s_1,s_2), \tag{B6}$$

where $\mathbf{u}_i=\mathbf{r}_i/(l_0\sqrt{2})$, and $\chi(s_1,s_2)$ is the spin part. The exact eigenvalues are given by

$$E_{NM,nm}=\hbar\omega_0(2N+|M|+1)+\varepsilon(n,|m|), \tag{B7}$$

where $\varepsilon(n,|m|)$ are the eigenvalues associated with the relative motion [see Eq. (B5)], (n,m) being the corresponding radial and azimuthal quantum numbers.

2. Pair correlation, electron density, and conditional probability distribution for the exact and sS-UHF two-electron wave functions

The bracket notation in Eqs. (3), (4), and (5) imply integrations over both the spatial and spin variables. In the case of the exact wave function Ψ given by Eq. (B6), the spin variables separate out, and thus $G(v)$, $n(v)$, and the CPD can be expressed as double integrals over the positions $(\mathbf{r}_1,\mathbf{r}_2)$ of the two-body spatial probability density $W(\mathbf{r}_1,\mathbf{r}_2)=|\Phi(\mathbf{r}_1,\mathbf{r}_2)|^2$, where Φ is the spatial part of Ψ. In particular, one finds

$$G(v)=2\pi\int\int\delta(\mathbf{r}_1-\mathbf{r}_2-\mathbf{v})W(\mathbf{r}_1,\mathbf{r}_2)d\mathbf{r}_1d\mathbf{r}_2 \tag{B8}$$

for the pair-correlation function,

$$n(v)=\int\int\sum_{i=1}^{2}\delta(\mathbf{v}-\mathbf{r}_i)W(\mathbf{r}_1,\mathbf{r}_2)d\mathbf{r}_1d\mathbf{r}_2 \tag{B9}$$

for the electron density, and

$$\mathcal{P}(\mathbf{v}|\mathbf{r}_2=\mathbf{v}_0)=\frac{W(\mathbf{v},\mathbf{r}_2=\mathbf{v}_0)}{\int d\mathbf{r}_1 W(\mathbf{r}_1,\mathbf{r}_2=\mathbf{v}_0)} \tag{B10}$$

for the conditional probability distribution.

In the case of the sS-UHF singlet ground state, the two electrons occupy two different spatial orbitals $\psi_1(\mathbf{r})$ and $\psi_2(\mathbf{r})$. Then the corresponding two-body wave function is the single determinant

$$\Psi^{\text{UHF}}(\mathbf{r}_1,\mathbf{r}_2)=\frac{1}{\sqrt{2}}[\psi_1(\mathbf{r}_1)\alpha(1)\psi_2(\mathbf{r}_2)\beta(2)$$

$$-\psi_1(\mathbf{r}_2)\alpha(2)\psi_2(\mathbf{r}_1)\beta(1)], \tag{B11}$$

where α and β denote the spin-up and down spinors, respectively. Integration of $|\Psi^{\text{UHF}}|^2$ over the spin variables yields the following two-body spatial probability density:

$$W^{\text{UHF}}(\mathbf{r}_1,\mathbf{r}_2)=\frac{1}{2}[|\psi_1(\mathbf{r}_1)|^2|\psi_2(\mathbf{r}_2)|^2+|\psi_1(\mathbf{r}_2)|^2|\psi_2(\mathbf{r}_1)|^2]. \tag{B12}$$

To calculate the conditional probability distribution in the case of the sS-UHF ground state, one replaces W by W^{UHF} in Eq. (B10).

[1] M.A. Kastner, Phys. Today **46(1)**, 24 (1993).

[2] R.C. Ashoori, Nature (London) **379**, 413 (1996).

[3] S. Tarucha, D.G. Austing, T. Honda, R.J. van der Hage, and L.P. Kouwenhoven, Phys. Rev. Lett. **77**, 3613 (1996).

[4] E.U. Condon and G.H. Shortley, *The Theory of Atomic Spectra* (Cambridge Univ. Press, London, 1935).

[5] D.R. Hartree, Proc. Cambridge Philos. Soc. **24**, 89 (1928).

[6] The failure of Bohr-type models, based on the orbiting of spatially correlated electrons in conjunction with the Bohr-Sommerfeld quantization rule, to yield a reasonable estimate of the ground state of the He atom signaled a looming crisis in physics in the 1920s, which Bohr himself, as well as others, had been keenly aware of, as summarized succintly by Sommerfeld: ''All attempts made hitherto to solve the problem of the neutral helium atom have proved to be unsuccessful'' [A. Sommerfeld, Rev. Sci. Instrum. **7**, 509 (1923)]. Also see A. Pais, *Niels-Bohr's Times* (Clarendon, Oxford, 1991), Chap 10; the review by J.H. Van Vleck, Philos. Mag. **44**, 842 (1922); M. Born, *The Mechanics of the Atom* (Ungar, New York, 1927). Subsequently, numerical solutions of the two-electron Schrödinger equation provided a quantitative resolution to the problem, but the first successful semiclassical treatment of the three-body Coulomb system did not occur untill 1980; see J.G. Leopold and I.C. Percival, J. Phys. B **13**, 1037 (1980); D. Wintgen, K. Richter, and G. Tanner, Chaos **2**, 19 (1992). Furthermore, based on rather general group-theoretical arguments arising from the observation of hierarchies with lower symmetry in the excited spectra, and motivated by ideas originating in nuclear-physics spectroscopy, it was discovered in the late 1970s and early 1980s that electron correlations in doubly excited He lead to a quantization of the spectrum much like in a linear triatomic molecule, e-He^{2+}-e. This molecular picture, with near rigidity and separability, results in ''infinite sequences of vibrational levels, on each of which is built an infinite sequence of rotational levels''; see M.E. Kellman and D.R. Herrick, Phys. Rev. A **22**, 1536 (1980); G.S. Ezra and R.S. Berry, *ibid.* **28**, 1974 (1983); S. Watanabe and C.D. Lin, *ibid.* **34**, 823 (1986). Interestingly, as in the aforementioned semiclassical treatments, the collinear configuration plays a special role in the moleculelike model, serving perhaps as a ''partial vindication'' of the geometry considered originally by Bohr.

[7] Å. Bohr and B.R. Mottelson, *Nuclear Structure* (Benjamin, Reading, MA, 1975).

[8] W. Nazarewicz, Nucl. Phys. A **574**, 27c (1994).

[9] C. Yannouleas and U. Landman, Phys. Rev. B **51**, 1902 (1995).

[10] W. Ekardt, *Metal Clusters* (Wiley, New York, 1999), Chaps. 1 and 4.

[11] In modeling of practical ''on-off'' (i.e., two-state) devices, one will undoubtedly have to take into account additional potential terms in the many-body Hamiltonian, such as those associated with image charges resulting from interfaces between different dielectric materials. The feasibility of constructing nanoscale logic cells via controlled manipulation of the antipodal arrangements of two electrons in a larger device, composed of four dots arranged in a square to form a quantum-dot supermolecule, is currently under intense experimental investigation; see I. Amlani, A.O. Orlov, G. Toth, G.H. Bernstein, C.S. Lent, and G.L. Snider, Science **284**, 289 (1999).

[12] E. Wigner, Phys. Rev. **46**, 1002 (1934).

[13] P.A. Maksym, Phys. Rev. B **53**, 10871 (1996).

[14] H.-M. Müller and S.E. Koonin, Phys. Rev. B **54**, 14 532 (1996).

[15] R. Egger, W. Häusler, C.H. Mak, and H. Grabert, Phys. Rev. Lett. **82**, 3320 (1999).

[16] C. Yannouleas and U. Landman, Phys. Rev. Lett. **82**, 5325 (1999).

[17] P. W. Anderson, *Basic Notions of Condensed Matter Physics* (Addison-Wesley, Reading, MA, 1984).

[18] D. J. Thouless, *The Quantum Mechanics of Many-Body Systems* (Academic Press, New York, 1972).

[19] H. Fukutome, Int. J. Quantum Chem. **20**, 955 (1981).

[20] For studies pertaining to the arrangement of classical point charges in a harmonic confinement, see Yu.E. Lozovik, Usp. Fiz. Nauk **153**, 356 (1987) [Sov. Phys. Usp. **30**, 912 (1987)]; V.M. Bedanov and F.M. Peeters, Phys. Rev. B **49**, 2667 (1994).

[21] That R_W is the only relevant parameter in the formation of a WM in a clean QD can be seen immediately from the exact Schrödinger equation describing the relative motion of two interacting electrons at $B=0$ in a parabolic confinement (Appendix B). Indeed, this equation when expressed in dimensionless variables as in Eq. (B5) contains R_W as the sole free parameter. The corresponding center-of-mass motion is independent of the interelectron repulsion. For how to extract information about the Wigner molecule from the exact two-body solution, see Sec. IV.

[22] B. Tanatar and D.M. Ceperley, Phys. Rev. B **39**, 5005 (1989).

[23] In all calculations, we used g^*(GaAs)$=-0.44$, m^*(GaAs)$=0.067m_e$, and $\hbar\omega_0=5$ meV, with $R_W=2.39$ (that is, $\kappa=8$); the same value of R_W is obtained by using κ(GaAs)$=12.9$ and $\hbar\omega_0=1.9$ meV, yielding the similar results given here, but with different absolute energy values.

[24] M. Wagner, U. Merkt, and A.V. Chaplik, Phys. Rev. B **45**, 1951 (1992).

[25] D. Pfannkuche, V. Gudmundsson, and P.A. Maksym, Phys. Rev. B **47**, 2244 (1993).

[26] M. Taut, J. Phys. A **27**, 1045 (1994).

[27] M. Taut, Phys. Rev. A **48**, 3561 (1993).

[28] M. Rontani, F. Rossi, F. Manghi, and E. Molinari, Phys. Rev. B **59**, 10 165 (1999).

[29] Here we differentiate between the exact solution of the Hamiltonian specified by Eqs. (1) and (2) from ''exact diagonalization methods'' of Hubbard-type Hamiltonians used as models of QD's [see, e.g., R. Berkovits, Phys. Rev. Lett. **81**, 2128 (1998)].

[30] The sS-UHF equations were solved using the Pople-Nesbet-Roothaan formalism; see *Modern Quantum Chemistry* (Ref. 31) p. 214. Also see J.A. Pople and R.K. Nesbet, J. Chem. Phys. **22**, 571 (1954). Apart from Ref. 16, the only previous use of a space-UHF method in QD's was in an investigation (see Ref. 14) of WM's but only for fully polarized QD's (i.e., under high magnetic fields where the spin unrestriction is not at play).

[31] A. Szabo and N.S. Ostlund, *Modern Quantum Chemistry* (McGraw-Hill, New York, 1989).

[32] E.K.U. Gross, E. Runge, and O. Heinonen, *Many-Particle theory* (Hilger, Bristol, 1991), Chap. 8.

[33] From the point of view of the terminology adopted here, the simple designation Hartree-Fock (HF) in the literature most often refers to the RHF method, in particular in atomic physics and the physics of the homogeneous electron gas. In nuclear physics, however, the simple designation HF most often refers to a space (S)-UHF method.

[34] See the article by Ezra and Berry in Ref. 6; also see R.S. Berry in *Structure and Dynamics of Atoms and Molecules: Conceptual Trends*, edited by J.L. Calais and E.S. Kryachko (Kluwer, Dordrecht, 1995) p. 155, and references therein.

[35] The orientational degeneracy of the sS-UHF solutions describing an electron molecule in a cirularly symmetric QD is a residue of the rotational invariance of the exact Hamiltonian, and naturally it suggests the possible emergence of a rovibrational spectrum associated with the excitations of the electron molecule. Depending on the value of the parameter R_W, the electron molecule may exhibit different degrees of ''rigidity,'' with electron molecules of high rigidity (forming for large R_W) exhibiting well-developed rovibrational bands; for the value of $R_W = 2.39$ used by us here, the electron molecule is rather ''floppy'' [C. Yannouleas and U. Landman, cond-mat/0003245]. Such rovibrational spectra can be described by several theoretical approaches, for example (i) at a more phenomenological level, by a quantization of the collective classical motions associated with the molecule, such as rotations, and bending and stretching vibrations [see Kellman and Herrick in Ref. 6 and Maksym in Ref. 13]; and (ii) at a microscopic level, by projecting the symmetry-broken HF determinant onto multideterminental wave functions with good angular momenta, thus restoring the symmetry of the exact Hamiltonian [P. Ring and P. Schuck, *The Nuclear Many-Body Problem* (Springer-Verlag, New York, 1980), Chap. 11; P.-O. Löwdin, in *Quantum Theory of Atoms, Molecules, and the Solid State*, edited by P.-O. Löwdin (Academic Press, New York, 1966), pp. 601–623. Furthermore, starting from an exact solution for the electrons in the QD, rovibrational characteristics can be obtained from the many-body eigenvalue spectra evaluated for different total angular momenta and spins in conjunction with an analysis of the conditional-probability densities (C. Yannouleas and U. Landman, cond-mat/0003245). We note that the *discrete* rovibrational collective spectra associated with symmetry-breaking in a QD may be viewed as finite analogs to the Goldstone modes accompanying symmetry breaking transitions in extended media (see Ref. 17).

[36] H.A. Jahn and E. Teller, Proc. R. Soc. London, Ser. A **161**, 220 (1937).

[37] Recall that for an electron moving in a 2D circularly symmetric potential the wave functions are given (in polar coordinates) by $\Psi_{n_r,m}(r,\theta) = R(r; n_r, |m|)\exp(im\theta)$ with corresponding energies $\mathcal{E}(n_r, |m|)$, where n_r is the number of radial nodes and m is the angular momentum quantum number, with $m = 0, \pm 1, \pm 2, \ldots$. In the JT framework, the second electron of the (open-shell) triplet state of the $2e$ QD occupies an orbital formed as a linear combination of the $n_r = 0$, $m = \pm 1$ states (denoted by p_+ and p_-), i.e., $p_x \propto p_+ + p_-$ or $p_y \propto p_+ - p_-$, with the one of lower energy being selected through the self-consistent distortion of the central mean field. As a consequence, the orbitals of both electrons in the $2e$ QD exhibit noncircular symmetry. The energy gain due to the JT distortion depends on the strength of the confinement potential, and it increases for weaker confinements. In natural atoms, the spontaneous JT effect is fairly small and

perturbative methods are usually adequate; see Chap. III.2 in *The Quantum Mechanics of Many-Body System* (Ref. 18).

[38] This cancellation of crystallization due to a strong-attractive-impurity effect is illustrated in Fig. 4(d), where the attractive impurity is able to capture two of the eight electrons in the dot. The two captured electrons form a singlet subunit and their orbitals are clearly circularly symmetric (see Appendix A).

[39] The effective confinement frequency $\Omega_{\text{eff}} = (\omega_0^2 + \omega_c^2/4)^{1/2}$ in the Darwin-Fock model of a 2D harmonically confined electron in the presence of a magnetic field B (where ω_0 is the frequency of the harmonic potential, and $\omega_c = eB/m^*c$ is the cyclotron frequency) increases as a function of the magnetic field; as a result, the Coulomb repulsion between the electrons increases. In a magnetic field, the energy of a harmonically confined electron is given in the Darwin-Fock model by $E_{n_r,m} = (2n_r + |m| + 1)\hbar\Omega_{eff} - m\hbar\omega_c/2$.

[40] Such JT-type electron molecules have been called Wigner molecules in previous publications treating fully polarized QD's (Refs. 13 and 14). However, this naming is not appropriate since their formation is not driven by the dominance of the interelectron repulsion (over the zero-point kinetic energy), which for large magnetic fields can be treated pertubatively (Refs. 24 and 26).

[41] Å. Bohr and B.R. Mottelson, Mat. Fys. Medd. Dan. Vidensk. Selsk. **27**, 16 (1953).

[42] S.G. Nilsson, Mat. Fys. Medd. K. Dan. Vidensk. Selsk. **29**, 16 (1955).

[43] V.M. Strutinsky, Nucl. Phys. A **95**, 420 (1967).

[44] For an early review of the application of Hartree-Fock methods to the description of open-shell, deformed nuclei, see G. Ripka, Adv. Nucl. Phys. **1**, 183 (1968).

[45] R.E. Peierls and J. Yoccoz, Proc. Phys. Soc., London, Sect. A **70**, 381 (1957).

[46] R.E. Peierls and D.J. Thouless, Nucl. Phys. **38**, 154 (1962).

[47] The concept of restoration of symmetry is not restricted to spatial symmetry, but includes also restoration of spin symmetry [see the paper by Löwdin in *Quantum Theory of Atoms, Molecules, and the Solid State* (Ref. 35)].

[48] G.E. Brown, *Unified Theory of Models and Forces* (North-Holland, Amsterdam, 1967), p. 64.

[49] For the purely parabolic confinement considered here, it turns out that the pair-correlation function reduces (Ref. 27) to the modulus square of the radial part of the wave function (see Appendix B) describing the relative motion, i.e., $G(v) = \Omega^2(v)/v$.

[50] See p. 620 of the paper by Löwdin mentioned in *Quantum Theory of Atoms, Molecules, and the Solid State* (Ref. 35) (in this paper the RHF solution is referred to as *conventional Hartree-Fock scheme*); this definition was also followed in Ref. 25, where a RHF solution was contrasted to the exact ground-state solution for two interacting electrons.

[51] C. Yannouleas and U. Landman (unpublished).